PERGAMON

Chaos, Solitons and Fractals 15 (2003) 327–341

CHAOS
SOLITONS & FRACTALS

www.elsevier.com/locate/chaos

Stabilizing periodic orbits in a chaotic semiconductor laser

E.F. Manffra [a,1], I.L. Caldas [a], R.L. Viana [b,*]

[a] *Instituto de Física, Universidade de São Paulo, Caixa Postal 66318, 05315-970 São Paulo, SP, Brazil*
[b] *Departamento de Física, Universidade Federal do Paraná, Caixa Postal 19081, 81531-990 Curitiba, Paraná, Brazil*

Accepted 12 November 2001

Abstract

We consider the single mode dynamics of a self-pulsating semiconductor laser model under modulated injection current. The observation of a chaotic regime for a wide range of parameters suggests the usefulness of this model for high-speed secure optical communications. A possible way to achieve symbol encoding by using such a laser as a light source is to control its chaotic dynamics. We study the stabilization of periodic orbits embedded in the chaotic invariant set of the system by applying perturbations on the amplitude of the injection current.

1. Introduction

Some of the advantages of semiconductor lasers are their wide wavelength coverage, compactness, high efficiency, power, lifetime and reliability; besides the fact that it is electrically pumpable [1]. Many semiconductor laser devices are found in a large variety of applications, from the miniature models used in laser pointers and CD players to state-of-the-art uses in high-speed optical communications. Of special relevance as light sources for digital communications are semiconductor lasers with wavelength constraints, such as vertical cavity surface emmiting lasers (VCSEL's) and distributed feedback lasers (DFB's), since their single mode operation is a requirement in long distance optical communication systems [2,3]. They typically have wavelength constraints which may cause a negative gain suppression factor and consequently a self- pulsating behavior [4,5]. These oscillations are preserved if a steady injection current is applied, but if the injection current is modulated, a more complex behavior is expected, like periodic orbits, quasiperiodic and chaotic behavior, and crises [6,7].

Chaotic behavior in diode lasers can be useful in the sense that we are able to encode and securely transmit information. In the first place one has to identify a chaotic attractor in the system, and analyze the free-running chaotic oscillations displayed by the uncontrolled laser source, in the presence of current injection [8]. Symbolic dynamics can be used to associate symbol sequences to the orbits embedded in the chaotic attractor in the state space. A given message is encoded if the chaotic trajectory is controlled by small and carefully chosen perturbations on a system parameter [9].

These controlling perturbations can steer the chaotic orbit to an unstable periodic orbit embedded in the attractor, and related to some symbolic sequence one desires to generate. The chaotic nature of the orbit is a key factor here, since the control is achieved by means of small perturbations, such that the laser system is only slightly affected by the external intervention. The encoded message is masked by the irregular nature of the chaotic oscillations and can be securely decoded by another system which is put in synchrony with the message source [10].

* Corresponding author. Tel.: +55-44-366-2323; fax: +55-41-267236.
E-mail address: viana@fisica.ufpr.br (R.L. Viana).
[1] Present address: Max-Planck-Institut fuer Physik Komplexer Systeme, Noethnitzer Strasse 38, 01187 Dresden, Germany.

0960-0779/03/$ - see front matter
PII: S0960-0779(01)00249-1

Chaos control in lasers has been extensively studied in recent years, as in a bulk cavity ring oscillator, used as a bistable resonator [11]; and in a single-mode CO_2 laser with an electro-optic feedback on the cavity losses [12]. Communication using chaos has been experimentally demonstrated by using electronic circuits [13,14], but these systems typically allow information transmitted at bandwidths in the kHz range. Chaotic laser sources, on the other hand, work at bandwidths of hundreds of MHz, hence at a much higher speed than electronic circuits [15]. This possibility has been verified using erbium-doped fiber ring lasers (EDFRL's), which operate in wavelengths for which the losses in the optical fibers are minimized [16]. In the latter experiment, the output beam was generated from a tunable semiconductor laser.

In this paper we explore the dynamical properties of semiconductor lasers with modulated injection current, in order to investigate the possibility of generating light waves with chaotic fluctuations of intensity for securely transmitting information using the richness of chaotic behavior. Firstly we make a dynamical characterization of chaotic motion through numerical integration of the single mode equations and analysis of the parameter space. In the second place we control the chaotic dynamics stabilizing embedded periodic orbits by using perturbations applied on an accessible system parameter.

Dynamical regimes in a semiconductor laser model with modulated current injection were reported in previous papers which emphasize the onset of self-pulsation [3,5], as well as its dynamical similarity with a class of one-dimensional circle maps [7]. It was found that chaotic dynamics can be achieved by many routes, as period-doubling cascades, type-I intermittency, and crisis-induced intermittency (chaos–chaos switchings). Chaos control will be numerically demonstrated in this paper using both the OGY method [9]and the inclusion of a second injection current source [17].

This paper is organized as follows: Section 2 introduces the model equations describing the behavior of the driven semiconductor laser model used in this work, and surveys some of its known dynamical properties. Section 3 presents results on a method of chaos suppression in this model, whereas in Section 4 we show periodic orbit stabilization using a feedback control technique. Section 5 contains our conclusions.

2. Diode laser model

Some types of semiconductor lasers as VCSEL's operate in single mode, a useful property for long-distance and high-speed communications [2,3]. This also reduces the number of equations to describe the diode laser behavior. In this case, the physical variables of interest are S, the density of laser photons, and N, the density of carriers. A two-dimensional vector field is formed by the rate equations for these variables, and the main source of non-linearity is represented by the cross products of S and N, present in both equations, the proportionality factors being related to the gains due to stimulated emission [18].

The wavelength constraints exhibited by diode lasers such as VCSEL's and DFB's give rise to a negative gain suppression factor [4]. This fact has been shown to be related to laser self-pulsation even under a steady injection current I_{DC} of carriers [5]. In the case where this injection is modulated with a given amplitude and frequency

$$I(\tau) = I_{DC} + I_{AC}\sin(\Omega\tau), \tag{1}$$

where τ is physical time, there may occur a more complex behavior, like mode-locking, quasiperiodic response, chaotic oscillations, and crises [3,6,7]. The non-linear response of self- pulsating laser diodes to externally injected optical signals has been used to investigate their synchronization properties [19].

In order to study these features far from the equilibrium, we shall consider a driven diode laser model with two rate equations for the photon and carrier densities, denoted by $S(\tau)$ and $N(\tau)$, respectively, and written as [5]

$$\frac{dN}{d\tau} = -\gamma(N - N_t)(1 - \epsilon S)S - k_n N + \frac{1}{\alpha}I(\tau), \tag{2}$$

$$\frac{dS}{d\tau} = \Gamma\gamma(N - N_t)(1 - \epsilon S)S - k_s S + k_n \Gamma\beta N, \tag{3}$$

where γ is the optical gain coefficient for stimulated emission, and k_n is the decay rate for spontaneous emission, equal to the inverse carrier lifetime ($k_n = 1/\tau_n$). Similarly, k_s is the decay rate due to loss of photons by effects like mirror transmission, scattering, etc.; and it is equal to the inverse of the photon lifetime ($k_s = 1/\tau_s$).

The other physical quantities in the above rate equations are: $I(\tau)$ is the injected current in the active region, α is the product of the electronic charge and the active volume region, β is the fraction of spontaneous emission in the lasing

Table 1
Values of the physical quantities for the semiconductor laser model [5]

Parameter	Value
τ_n	1.49 ns
τ_p	3.89 ps
α	1.58×10^{-35} A m^3 s
Γ	0.986
β	1.0×10^{-5}
N_t	9.26×10^{23} m^{-3}
γ	8.69×10^{-13} m^3 s^{-1}
ϵ	-2.2×10^{-23} m^{-3}

mode, N_t is the carrier density required for transparency, ϵ is the gain suppression factor, and Γ is the mode confinement factor. The values for these parameters which are to be used in the forthcoming numerical simulations are given in Table 1.

The distinctive feature of this model is the presence of a negative gain suppression factor ($\epsilon < 0$), what opens the possibility of self-pulsation. This model was first investigated by Bennett et al. [5], through a linear stability analysis, confirming the onset of self-pulsations due to the lack of relaxation oscillation damping, as well as the possibility of chaotic oscillations. Some of the dynamical regimes found in this work were further studied in a previous paper [7], where we investigated the existence of type-I intermittency and crisis-induced intermittency (chaos– chaos switchings) in the dynamics of this model.

For convenience of numerical analysis, we define normalized variables as follows

$$x_1 = |\epsilon|N, \quad x_2 = |\epsilon|S, \quad t = \frac{\tau}{\tau_n}, \tag{4}$$

as well as the non-dimensional parameters

$$\mathcal{J}(t) = \frac{I(t)\tau_n|\epsilon|}{\alpha}, \quad C = \frac{\gamma\tau_n}{|\epsilon|}, \quad D = |\epsilon|N_t, \quad E = \frac{\tau_n}{\tau_p}, \quad F = \Gamma\beta, \quad G = \frac{\epsilon}{|\epsilon|}, \quad H = \Gamma D, \tag{5}$$

so that the model equations are rewritten in the form

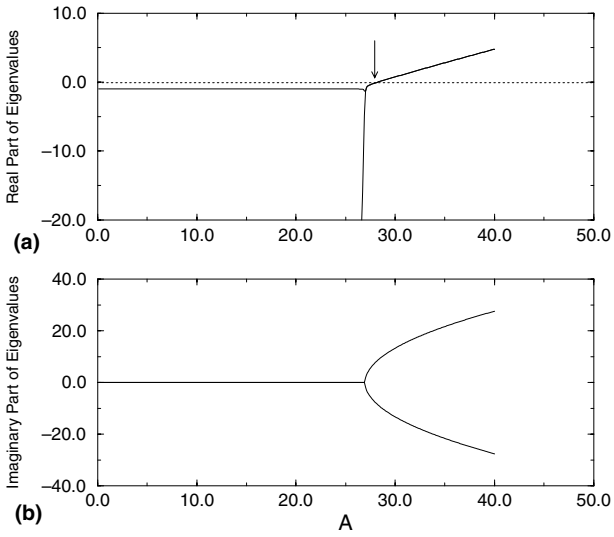

Fig. 1. Dependence of the (a) real part, and (b) imaginary part of the eigenvalues for the linearized system around the equilibrium solutions of Eqs. (6) and (7), on the steady injection current A. The arrow indicates the point where a Hopf bifurcation occurs, at $A_H = 28.21$.

$$\dot{x}_1 = -x_1 - C(x_1 - D)(1 - Gx_2)x_2 + \mathcal{J}(t), \tag{6}$$

$$\dot{x}_2 = Fx_1 - Ex_2 + H(x_1 - D)(1 - Gx_2)x_2, \tag{7}$$

where the normalized current injection is given by

$$\mathcal{J}(t) = A + B\sin(Wt) \tag{8}$$

with A and B being the corresponding DC and AC amplitudes, respectively, and W the modulation frequency.

The steady injection case ($A \neq 0,\ B = 0$) for small values of A has as the equilibrium point a stable node, that undergoes a supercritical Hopf bifurcation for $A = A_H \approx 28.21$, for the parameters listed in Table 1. This can be inferred from the behavior of the real (Fig. 1(a)) and imaginary (Fig. 1(b)) parts of the eigenvalues of the Jacobian matrix related to Eqs. (6) and (7), and evaluated at the equilibrium points. For A-values not far from A_H there is a stable limit cycle. In Fig. 2 we show such an attractor for the case $A = 40.44 > A_H$, as well as two trajectories from different initial conditions which asymptote to it. The time rate of change of the phase at the limit cycle is a "natural" frequency found to be $W_0 = 11.70$, physically representing a laser self-pulsation with frequency 1.25 GHz. From now on, we shall fix the DC-part of the injection current amplitude at this value.

If a modulated injection current in the form (8) is applied, the dynamics becomes of a periodically driven limit-cycle oscillator. When the dissipation is strong enough, its dynamics is similar to that of a one- dimensional circle map [20,21]. In fact, we observe in the modulation parameter space (B versus W/W_0) a structure akin to that displayed by a sine-circle map, as depicted in Fig. 3, where the maximal Lyapunov exponent λ_1 is plotted in grayscale. The darker the pixel, the lesser is the exponent.

For small modulation amplitudes we have the Arnold tongues corresponding to the mode-locking regions anchored, on the $B = 0$ axis, at harmonics of the natural frequency W_0, i.e., at $W = nW_0$, with $n = 1, 2, 3, \ldots$ [22]. The darker lines inside the tongues indicate superstable orbits, for which the exponent diverges to minus infinity. These Arnold tongues are intertwined with quasi-periodic regions, for which the ratio W/W_0 is an irrational number. These tongues start to overlap for higher B-values, when the corresponding one-dimensional dynamics is no longer invertible, and there result regions of chaotic dynamics (the bright regions in Fig. 3) mixed with multistable periodic and quasiperiodic ones.

In Fig. 4(a) we depict such a chaotic attractor, where we have picked up a point in the Lyapunov plot of Fig. 3 at $B = 29.03$ and $W = 37.44 = 3.2W_0$. This figure results from a stroboscopic, or time-T map, where $T = 2\pi/W$ is the period of the external injection current. The fractal nature of this attractor is apparent when a particular region of it is enlarged (Fig. 4(b)), showing a self-similar band structure with folds due to homoclinic crossings between stable and unstable manifolds.

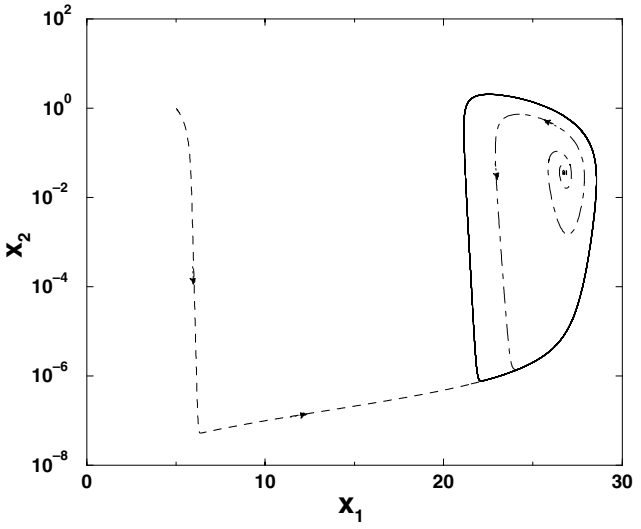

Fig. 2. Limit cycle in the phase plane (x_1, x_2) for $A = 40.44$. Dotted lines represent two trajectories, starting from different initial conditions, that asymptote to the attractor.

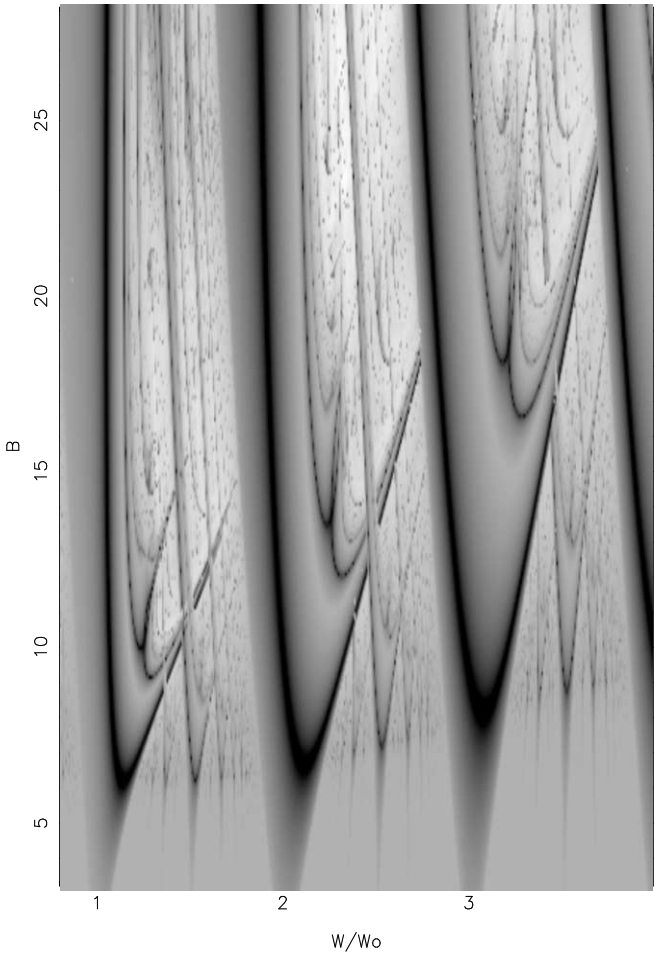

Fig. 3. Lyapunov plot of a region of the modulation parameter space (B versus W) for the laser diode model. The maximal exponent is represented in grayscale, for which the larger the exponent the brighter is the corresponding pixel.

3. Suppression of chaos

Suppression of chaos due to weak periodic perturbations applied on an externally driven oscillator has been proposed by Braiman and Goldhirsch [17], where an AC-driven Josephson junction equation is considered. There was added a weak external sinusoidal forcing, beside the main driving. Many interesting features were observed: (i) the elimination of chaotic dynamics, or at least a decrease in the maximal Lyapunov exponent; (ii) the stabilization of narrow subharmonic steps; and (iii) a non-monotonic behavior of the winding number as a function of the control parameters. Earlier works have proved that stabilization of periodic orbits is also possible by the application of external periodic forcing at resonant frequencies [23,24].

For a chaotic attractor, like that shown in Fig. 4, there is an infinite number of embedded unstable periodic orbits [25]. Since our system is a non-autonomous one, these periodic orbits are harmonic or subharmonic responses to the external forcing, representing laser pulsations of periods equal to integer multiples of $T = 2\pi/W$. In principle, any of these orbits is stabilizable and, in fact, the following section illustrates a control method for stabilizing some desirable orbit from a large number of choices. Applying a second and weak periodic perturbations is equivalent to let the system choose by itself what is the periodic orbit it wants to settle down in, for a given forcing amplitude.

For our laser diode system this strategy consists on the addition of a second weak current injection source, with a small amplitude K, when compared with the main driving, and a frequency mismatch b

$$\mathcal{J}(t) \to A + B\sin(Wt) + J\sin(bWt), \tag{9}$$

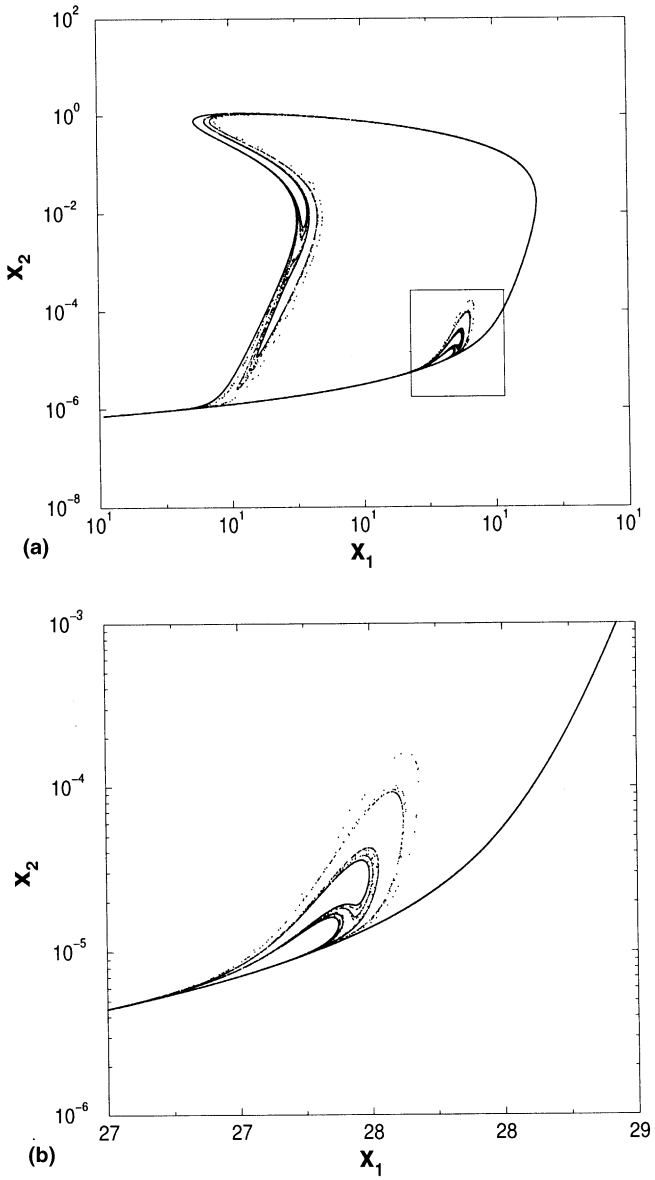

Fig. 4. (a) Poincaré (stroboscopic) map for Eqs. (6) and (7) with $A = 40.44$, $B = 29.03$, and $W = 37.44$. (b) Enlargement of the small box depicted in (a).

where it is required that $J \ll B$. In principle the frequency mismatch may be any real number in the $[0, 1]$ interval, but if b is an irrational number it follows that the system is quasiperiodically forced. In this case it was proved that there may appear strange (i.e., fractal) but non-chaotic attractors [26].

We analyzed the effects of applying this second current source to the system for parameters leading to the chaotic attractor depicted in Fig. 4. The values of J and b have been chosen to steer the chaotic trajectory to some embedded periodic orbit, which amounts to stabilize this orbit. Let us fix the frequency mismatch to a rational value $b = 0.4$ and vary the second amplitude J. In Fig. 5(a) we depict the corresponding bifurcation diagram for the phase-space coordinate x_1, with the related maximal Lyapunov exponent being shown in Fig. 5(b). It follows that we can suppress chaotic behavior when $J > J_c \approx 2.67$ for a relatively large window, with chaotic bands showing up again for $J \gtrsim 4.20$. Since J_c is $\approx 9\%$ of B, one is able to suppress chaos with a rather weak current source, mismatched in frequency with the main driving. As an illustrative example, in Figs. 6(a) and (b) we show examples of phase portraits for uncontrolled

($J = 0$) and controlled attractors, respectively, when $J = 2.77 > J_c$. The latter case corresponds to a period-5 orbit that has been stabilized by the perturbation.

To investigate what is the influence of the frequency mismatch b on taming the chaotic dynamics, we present in Fig. 7 a Lyapunov plot of a region in the parameter plane (J versus b) of the second periodic source. As in Fig. 3, the darker the pixel, the smaller the value of the maximal Lyapunov exponent. Black pixels, accordingly, indicate negative values for it, corresponding to states for which chaos has been suppressed. There are a few isolated regions of stability, embedded in a predominantly chaotic sea.

4. Stabilizing periodic orbits

A disadvantage of the previous control scheme is the difficulty on choosing the period of the orbit to be stabilized for a given value of the perturbation parameter. For example, for the case depicted in Fig. 6 the only stabilizable orbits have periods higher than five and, even so, the higher periods are quite difficult to resolve for there is a period-doubling

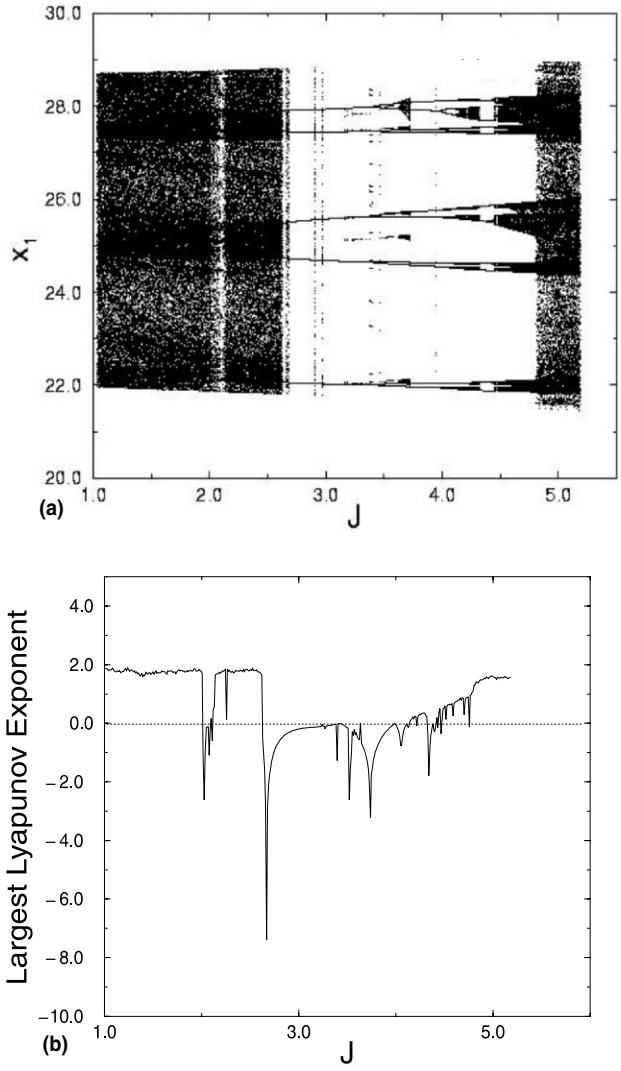

Fig. 5. (a) Bifurcation diagram of x_1 as a function of the second current injection amplitude J, for $b = 0.4$. The remaining parameters are the same as in Fig. 4. (b) Maximal Lyapunov exponent versus J.

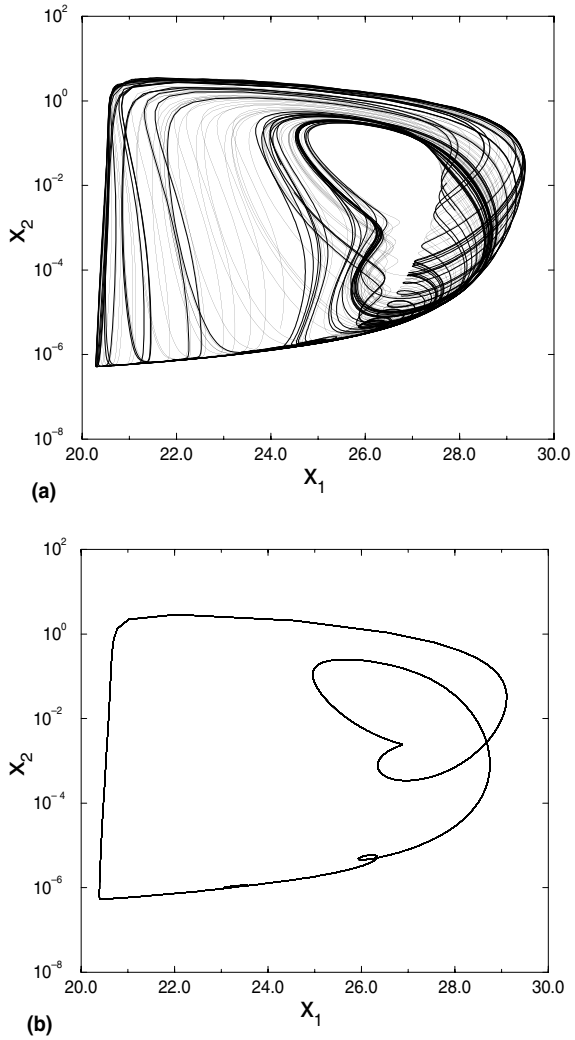

Fig. 6. (a) Phase portrait of the chaotic attractor for the same parameters as in Fig. 4. (b) Controlled periodic orbit obtained with a second current source with $J = 2.77$ and $b = 0.4$.

cascade with a fast accumulation of bifurcations. If we would like to obtain a period- 1 orbit, for example, a thorough investigation of the parameter plane should be made in order to find a pair of values (J, b) that would steer chaotic oscillations to this periodic orbit. This is clearly a time-consuming task, and may be impracticable in an experiment.

In order to be able to choose what periodic orbit we would like to stabilize, we need a feedback scheme that teach us a control law for the necessary perturbation values. One of such feedback control methods uses a linearization of the dynamics in a small neighborhood of the periodic orbit one wants to stabilize, and derives a control law giving the value of the perturbation which, when applied to an accessible parameter, directs a chaotic trajectory to the stable manifold of a perturbed periodic orbit [9]. The ergodic nature of the dynamics is then invoked to ensure that the approach to a periodic orbit embedded in the chaotic attractor occurs for a time interval that scales with the size of the neighborhood chosen. In this way we are able to stabilize any embedded periodic orbit by applying only small perturbations [27]. This technique is particularly important in communication applications, where we may want to encode some symbolic sequence in a chaotic signal by making only small perturbations on a system parameter [8].

We shall briefly outline the basics of this technique. Let a N-dimensional map be written as

$$\mathbf{z}_{n+1} = \mathbf{F}(\mathbf{z}_n, p), \tag{10}$$

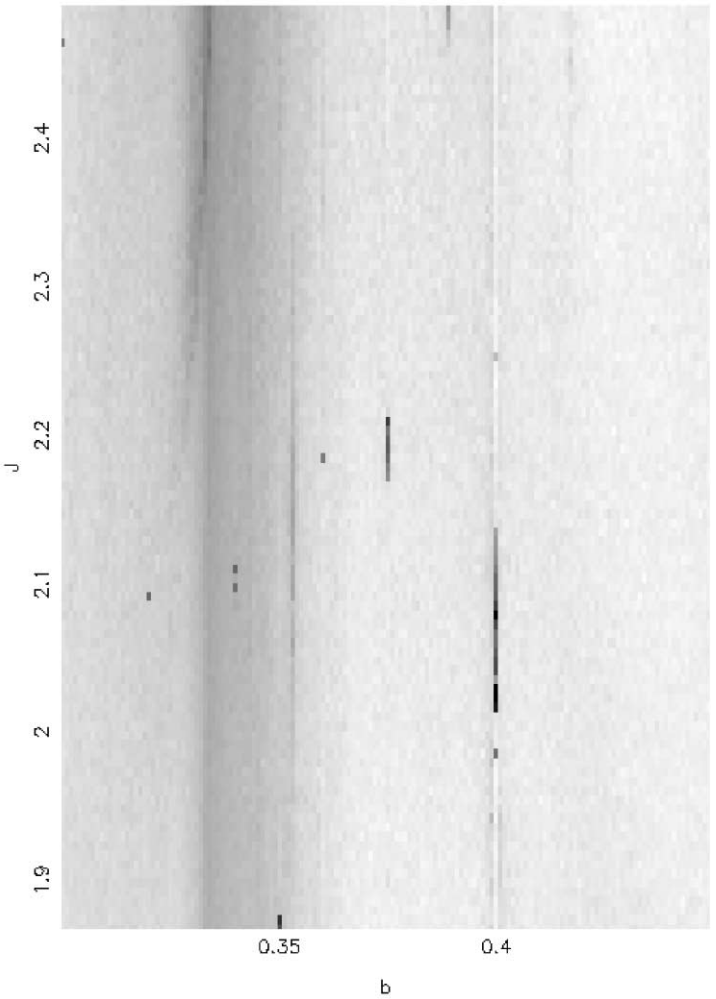

Fig. 7. Lyapunov plot of a region of the modulation parameter space for the second injection current. The grayscale is the same as in Fig. 3, and the parameters are the same as in Fig. 4.

where $\mathbf{z} \in \mathbb{R}^N$, and $p \in \mathbb{R}$ is a control parameter that can be externally perturbed. If the original dynamical system is a periodically driven continuous time flow, as in the diode laser model with modulated current injection, **F** can be regarded as the time-T stroboscopic map.

Suppose that for a value $p = \bar{p}$ of the control parameter there exists a chaotic attractor of the system. In principle any of the embedded periodic orbits can be chosen to be stabilized by using small perturbations on p. We choose the orbit that would give us the desired performance. By a small perturbation we mean that we restrict the (time-dependent) p-values to lie in some small interval

$$|p_n - \bar{p}| < \delta, \tag{11}$$

where $|\delta/\bar{p}| \ll 1$, and if p_n is outside this interval we consider $p_n = \bar{p}$ [28].

To understand how an arbitrary periodic orbit can be stabilized by this technique, let us consider a small neighborhood of size ε of the periodic orbit to be stabilized. In this neighborhood the system **F** is approximately linear, and the orbit is stabilizable by feedback control [29]. A typical chaotic trajectory in the attractor eventually enters the neighborhood of the desired periodic orbit, regardless of how small ε is. Once this occurs, we apply perturbations according to a *linear* control law and keep the trajectory close to the chosen periodic orbit.

The time interval for entering in such a neighborhood is also the length of a chaotic transient orbit. The average time to achieve control $\langle\tilde{\tau}\rangle$ was found to scale algebraically with the maximum allowed perturbation δ: $\langle\tilde{\tau}\rangle \sim \delta^{-\gamma_1}$ [9]. The

exponent γ_1 is related to the stable and unstable eigenvalues of the periodic orbit being controlled, for two-dimensional diffeomorphisms [30]. This method is rather robust to external noise, since every time a trajectory is kicked off the controlled orbit, it turns out that the control is reactivated, bringing the trajectory back to the desired orbit.

The periodic orbit to be stabilized can be an unstable fixed point $\mathbf{z}^*$ of the map (10) or a point belonging to a period-q cycle. In the latter case it is a fixed point of the q-times iterated map. Writing $\mathbf{z}^*(\bar{p})$ means that this orbit is embedded in the chaotic attractor that exists for $p = \bar{p}$. If the ε-neighborhood is small enough, and the values of the control parameter p_n are close to the $\bar{p}$, we can linearize the map (10) in both $\mathbf{z}$ and p variables:

$$\mathbf{z}_{n+1} - \mathbf{z}^*(\bar{p}) = \mathbf{M}(\mathbf{z}_n - \mathbf{z}^*(\bar{p})) + \mathbf{N}(p_n - \bar{p}), \tag{12}$$

where

$$\mathbf{M} = \left.\frac{\partial \mathbf{F}}{\partial \mathbf{z}}\right|_{\mathbf{z}^*(\bar{p}),\bar{p}}, \quad \mathbf{N} = \left.\frac{\partial \mathbf{F}}{\partial p}\right|_{\mathbf{z}^*(\bar{p}),\bar{p}} \tag{13}$$

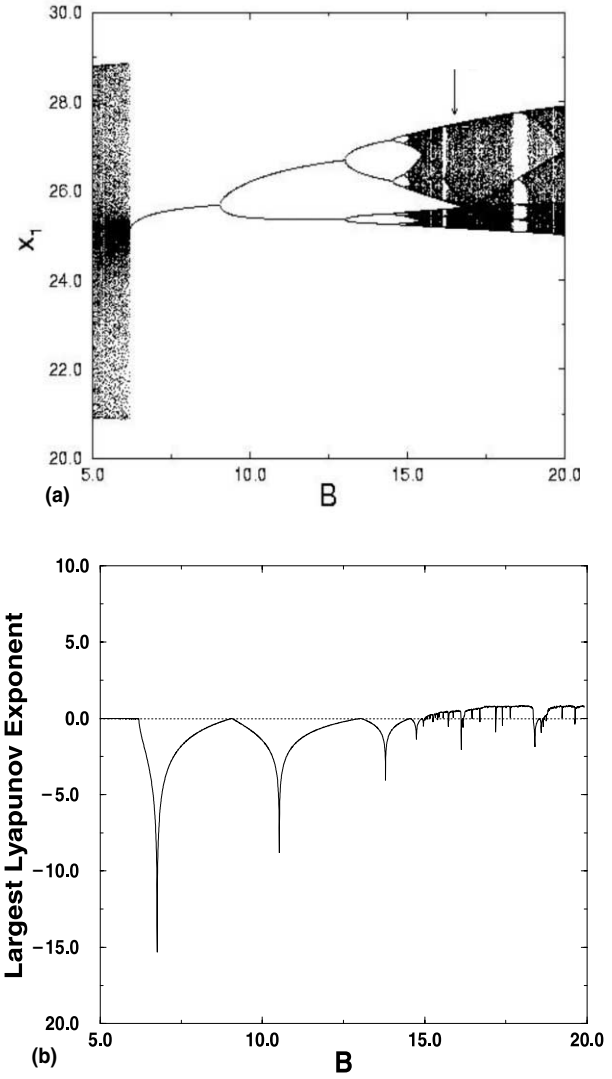

Fig. 8. (a) Bifurcation diagram for x_1 as a function of the current amplitude B, for $A = 40.44$ and $W = 14.04$. The arrow indicates the value $B = \bar{B} = 16.86$, for which the system has a chaotic orbit to be controlled. (b) Maximal Lyapunov exponent versus B.

are the $N \times N$ Jacobian matrix and a column matrix of derivatives with respect to the control parameter, respectively, evaluated at the periodic orbit and at $\bar{p}$.

Likewise, we assume a linear control law for the parameter p in the form

$$p_n - \bar{p} = -\mathbf{K}^{\mathrm{T}}(\mathbf{z}_n - \mathbf{z}^*(\bar{p})), \tag{14}$$

where $\mathbf{K}$ is a row matrix with entries chosen so that the fixed point $\mathbf{z}^*(\bar{p})$ is stabilized under the perturbation. Inserting (14) into (12) we have

$$\mathbf{z}_{n+1} - \mathbf{z}^*(\bar{p}) = (\mathbf{M} - \mathbf{N}\mathbf{K}^{\mathrm{T}})(\mathbf{z}_n - \mathbf{z}^*(\bar{p})), \tag{15}$$

so that $\mathbf{z}^*(\bar{p})$ will be stable if the matrix $\mathbf{M} - \mathbf{N}\mathbf{K}^{\mathrm{T}}$ has eigenvalues with modulus less than unity. This can be done by choosing appropriate values for the elements of the matrix $\mathbf{K}$. A standard technique for this problem is the pole placement one [31].

For the semiconductor laser model focused in this work we have $\mathbf{z}_n = (x_{1n}, x_{2n})^{\mathrm{T}}$, where x_{1n} and x_{2n} are the normalized carrier and photon densities, respectively, sampled at times $t = n(2\pi/W)$, with integer n. Moreover, we will use the external injection current amplitude B as the control parameter p. We shall fix the injection current frequency at

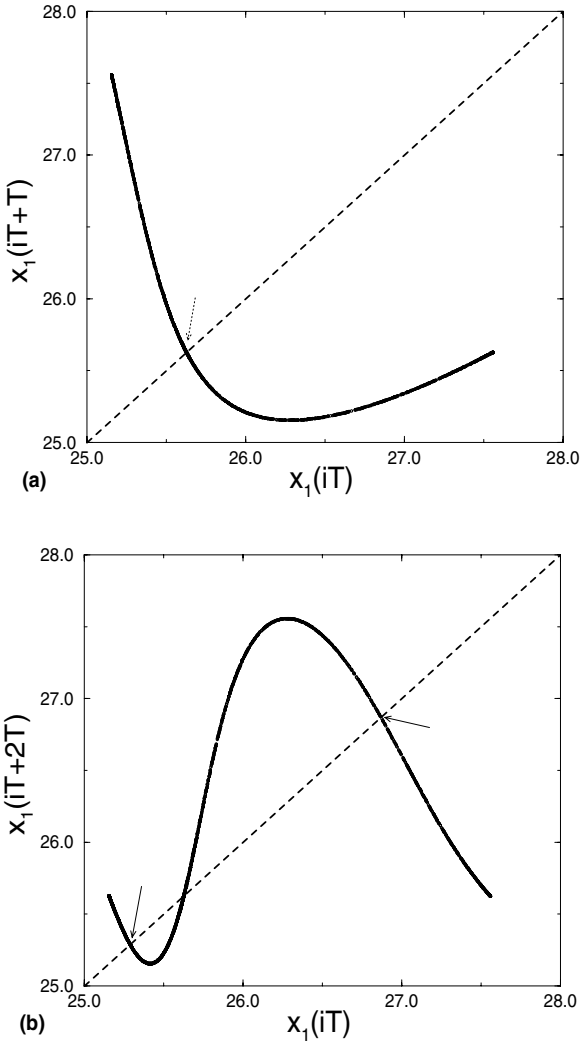

Fig. 9. (a) First and (b) Second return maps of x_1 for $B = \bar{B} = 16.86$ and the same remaining parameters as in Fig. 8. The arrows indicate the orbits that are to be stabilized.

Table 2
Some unstable low-period orbits embedded in a chaotic attractor for $A = 40.44$, $W = 14.04$, $B = 16.86$, and the corresponding values of the derivatives **M** and **N** defined by Eq. (13)

Period	Orbit points (x_1^*, x_2^*)	**M**	**N**
1	$(25.62, 2.62 \times 10^{-6})$	−2.11	−196.91
2	$(25.28, 2.19 \times 10^{-6})$	−1.95	−237.76
.	$(26.86, 6.93 \times 10^{-6})$	−1.96	−67.44

$W = 14.04 \approx 1.2W_0$, since it is near a 1/1 mode-locking region (see Fig. 3), in the vicinity of which there are a large number of low-period orbits to be controlled. In Figs. 8(a) and (b) we present a $x_{1n} - B$ bifurcation diagram for the time-T map, along with the corresponding maximal Lyapunov exponent. There are quite large intervals of B for which we have chaotic dynamics. We choose the injection current amplitude value $\bar{B} = \bar{p} = 16.86$ (indicated by an arrow in Fig. 8(a)) for which the system has a chaotic attractor.

Previous works [5,7] have indicated that, for a wide portion of the modulation parameter space $(B - W)$, the dynamics of (6) and (7) is similar to that of a non-linear circle map. This is further supported by the fact that the second Lyapunov exponent (λ_2) for the laser diode system remains between −55 and −80, what indicates a strongly dissipative

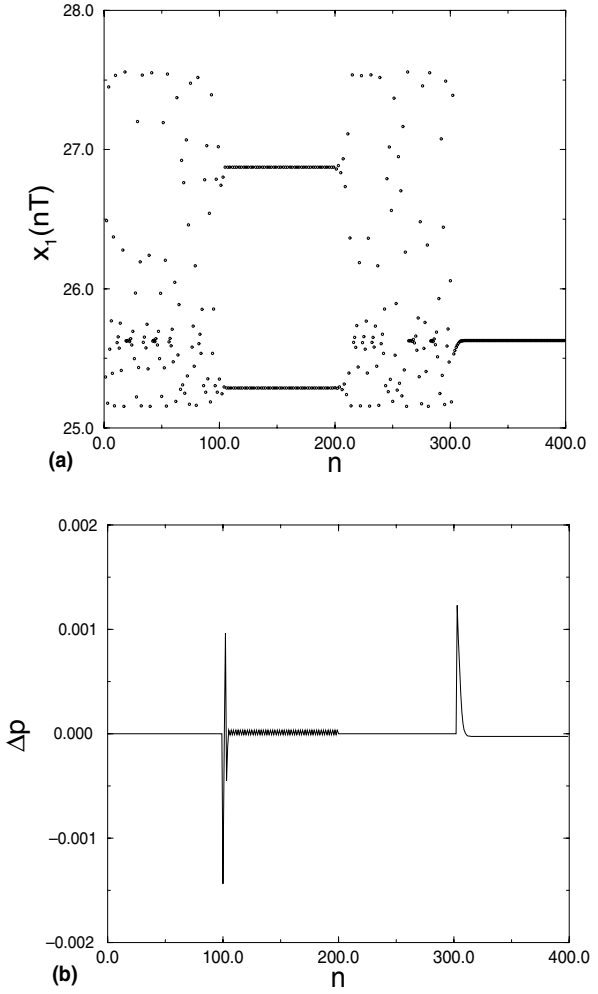

Fig. 10. (a) Time series for the stroboscopic map of x_1 showing the stabilization of period-2 and period-1 orbits. (b) Corresponding values of the parameter perturbation $\delta p = \delta B = B_n - \bar{B}$. The remaining parameters are the same as in Fig. 9.

system, in such a way that the dynamics is effectively one-dimensional [7]. We shall use this fact to simplify the application of the OGY control technique. In this case the state vector **z** is one of the coordinates, say x_1, and the matrices **M** and **N** reduce to scalar derivatives.

Our goal is to stabilize an unstable fixed point and a period-2 orbit embedded in the chaotic attractor at $B = \bar{B}$. These orbits were numerically determined from the first and second return maps for the x_1 coordinates of the time-T stroboscopic map, respectively (Figs. 9(a) and (b)). The results are presented in Table 2, where we also indicate the values of the derivatives **M** and **N** that were numerically obtained through least-squares fits using points in the neighborhood of these unstable orbits.

We apply parameter perturbations on the injection current amplitude according to the technique described in this section. Fig. 10(a) shows the stabilization of both the fixed point and the period-2 orbits, for different times. In Fig. 10(b) we depict the corresponding values of the perturbation needed: $\delta p = \delta B = B_n - \bar{B}$. The time to achieve control, once the perturbation is switched on, is very short for both orbits, indicating that we do not need to use targeting techniques [32,33] to increase the efficiency of control for this system. Figs. 11(a) and (b) show phase portraits of the continuous time laser diode model for the two controlled orbits shown by Fig. 10. In the background we depict the chaotic attractor where the periodic orbits came from.

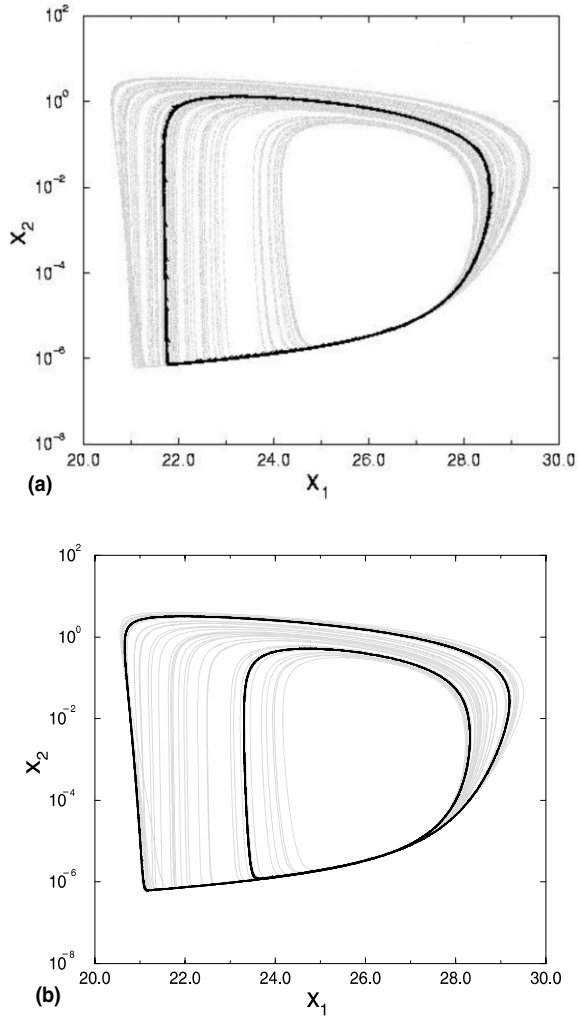

Fig. 11. Poincaré (stroboscopic) maps for (a) period-1 and (b) period-2 orbits stabilized. In background we depict the chaotic attractor in which these orbits were embedded.

5. Conclusions

High-speed telecommunication using fiber-optic networks demands the use of semiconductor lasers. Secure information transmission would require a laser source that is able to respond to small perturbations in an accessible parameter. This is the reason we have chosen a single mode laser diode model with current injection, since the latter is an experimentally feasible way to generate a signal in which we encode some symbolic sequence. To achieve this goal we need to identify, characterize, and control chaotic dynamics in this system. In this paper we aimed to accomplish the latter task.

Two control strategies were used. In the first, a second applied current source is applied to the system with the purpose of either to suppress chaos or decrease the leading Lyapunov exponent. The second scheme uses a feedback mechanism to design the application of small perturbations on a system parameter, in our case the amplitude of the injected current, to stabilize periodic orbits embedded in a chaotic attractor of the system.

The first technique would be useful to suppress chaos when it is undesirable for some practical reason, for example a large signal-to-noise ratio. It is a rather easy technique to implement experimentally, since the same physical mechanism responsible to the main injected current source can be used to generate a second weak signal. However, it does not allow an easy choice of the orbit to which we want to steer the chaotic trajectory. We have used this technique to stabilize a chaotic trajectory to a period-5 orbit by using a second source with less than 10% of the main source amplitude.

On the other hand, the OGY chaos control method takes advantage from the fact that the system is chaotic, and use its inherent flexibility to stabilize trajectories of arbitrary period. It involves a feedback mechanism that demands some high-speed and low-power electronics and is quite robust with respect to external noise.

We have demonstrated the usefulness of the OGY method for stabilizing orbits of periods one and two, embedded in a chaotic orbit. The control parameter was the amplitude of the injected current. The maximum perturbation strengths needed in the case studied were less than 0.01% of the injected current amplitude. Hence, it involves the use of very small perturbations, when compared with the main source of external driving. In principle, the price to pay for such a smallness would be a large time to achieve control, but if this happens we can resort to targeting techniques to decrease this transient length to a value that is experimentally reasonable.

Acknowledgements

This work was made possible through partial financial support from the following Brazilian government agencies: FAPESP, CAPES, CNPQ, Fundação Araucária, and FUNPAR.

References

[1] Chow WW, Koch S, Sargent M. Semiconductor laser physics. New York, Berlin, Heidelberg: Springer; 1994.
[2] Kawaguchi H. Optical bistability and chaos in a semiconductor laser with a saturable absorber. Appl Phys Lett 1984;45:1264–6.
[3] Winful HG, Chen YC, Liu AM. Frequency locking, quasi-periodicity, and chaos in modulated self-pulsing semiconductor lasers. Appl Phys Lett 1986;48:616–8.
[4] Wang G, Nagarajan R, Tauber D. Reduction of damping in high-speed semiconductor lasers. IEEE Phot Tech Lett 1993;5:642–5.
[5] Bennett S, Snoweden CM, Iezekiel S. Effect of negative gain suppression on the stability of laser diodes. Appl Phys Lett 1995;66:1874–6.
[6] Juang C, Chen MR, Juang J. Nonlinear dynamics of self-pulsating laser diodes under external drive. Opt Lett 1999;24:1346–8.
[7] Manffra EF, Caldas IL, Viana RL, Kalinowski, HJ. Type-I intermittency and crises-induced intermittency in a semiconductor laser under injection current modulation. Nonlinear Dyn (to be published).
[8] Hayes S, Grebogi C, Ott E. Communicating with chaos. Phys Rev Lett 1993;70:3030–4.
[9] Ott E, Grebogi C, Yorke JA. Controlling chaos. Phys Rev Lett 1990;64:1196–9.
[10] Cuomo KM, Oppenheim AV. Circuit implementation of synchronized chaos, with applications to communications. Phys Rev Lett 1993;71:65–8.
[11] Lynch S, Steele AL. Controlling chaos in nonlinear optical resonators. Chaos, Solitons & Fractals 2000;11:721–8.
[12] Ciofini M, Labate A, Meucci R, Arecchi FT. Experimental control of chaos in a delayed high-dimensional system. Eur Phys J D 1999;7:5–9.
[13] Hayes S, Grebogi C, Ott E, Mark A. Experimental control of chaos for communication. Phys Rev Lett 1994;73:1781–4.
[14] Li HJ, Chern JL. Coding the chaos in a semiconductor diode for information transmission. Phys Lett A 1995;206:217–21.
[15] Hohl A, Van der Linden JC, Roy R. Determinism and stochastic of power-dropout events in semi-conductor lasers with optical feedback. Opt Lett 1995;20:2396–8.
[16] Van Wiggeren GD, Roy R. Communication with chaotic lasers. Science 1998;279:1198–200.

[17] Braiman Y, Goldhirsch I. Taming chaotic dynamics with weak periodic perturbations. Phys Rev Lett 1991;66:2545–8.
[18] Milonni PW, Eberly JH. Lasers. New York: Wiley; 1988.
[19] Egan A, Harley-Stead M, Rees P, Lynch S, McEvoy P, O'Gorman J, Hegarty A. All-optical synchronization of self-pulsating laser diodes. Appl Phys Lett 1996;68:3534–6.
[20] Ding EJ. Analytical treatment of a driven oscillator with a limit cycle. Phys Rev A 1987;35:2669–83.
[21] Ding EJ. Structure of the parameter space for a prototype nonlinear oscillator. Phys Rev A 1987;36:1488.
[22] Baptista MS, Caldas IL. Phase-locking and bifurcations of the sinusoidally-driven double scroll circuit. Nonlinear Dyn 1998;17:119–39.
[23] Bryant P, Wiesenfeld K. Suppression of period-doubling and nonlinear parametric effects in periodically perturbed systems. Phys Rev A 1996;33:2525–46.
[24] Lima R, Pettini M. Suppression of chaos by resonant parametric perturbations. Phys Rev A 1990;41:726–33.
[25] Grebogi C, Ott E, Yorke JA. Unstable periodic orbits and the dimension of multifractal chaotic attractors. Phys Rev A 1988;37:1711–24.
[26] Kapitaniak T, Wojewoda J. Attractors of quasiperiodically forced systems. Singapore: World Scientific; 1994.
[27] Kapitaniak T. Controlling chaos: theoretical and practical methods in non-linear dynamics. New York: Academic Press; 1996.
[28] Grebogi C, Lai YC. Controlling chaotic dynamical systems. Syst Contr Lett 1997;31:307–12.
[29] Ogata K. Modern control engineering. 2nd ed. Englewood Cliffs, NJ: Prentice-Hall; 1990.
[30] Grebogi C, Ott E, Yorke JA. Controlling chaotic dynamical systems. In: Campbell D, editor. CHAOS/XAOC, Soviet-American Perspectives on Nonlinear Dynamics. New York: American Institute of Physics; 1990.
[31] Romeiras FJ, Grebogi C, Ott E, Dayawansa WP. Controlling chaotic dynamic systems. Physica D 1992;58:165–92.
[32] Shinbrot T, Grebogi C, Ott E, Yorke JA. Using the sensitive dependence of chaos (the butterfly effect) to direct trajectories in an experimental chaotic system. Phys Rev Lett 1992;68:2863–6.
[33] Baptista MS, Caldas IL. Easy-to-implement method to target nonlinear systems. Chaos 1998;8:290–9.